

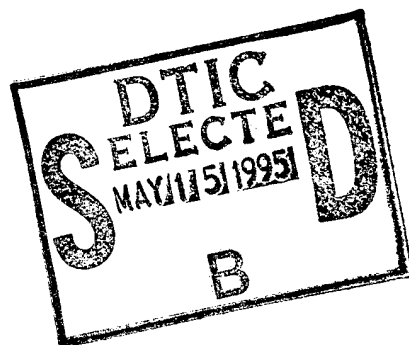
# NATIONAL AIR INTELLIGENCE CENTER



USING OPTICAL INTERFERENCE METHODS TO MEASURE  
ACOUSTO-OPTICAL DEVICE THERMAL EFFECTS

by

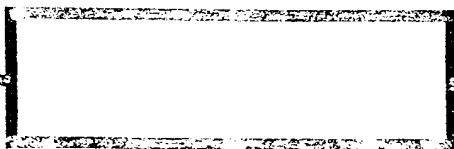
Xu Binghuo, Zhao Guozhen



19950512 079

DTIC QUANTITY INSPECTED 8

Approved for public release;  
Distribution unlimited.



NAIC- ID(RS)T-0398-94

**HUMAN TRANSLATION**

NAIC-ID(RS)T-0398-94

5 April 1995

MICROFICHE NR: 950000170

USING OPTICAL INTERFERENCE METHODS TO MEASURE  
ACOUSTO-OPTICAL DEVICE THERMAL EFFECTS

By: Xu Binghuo, Zhao Guozhen

English pages: 11

Source: Yingyong Shengxue, Vol. 8, Nr. 6, November 1989;  
pp. 19-23

Country of origin: China

Translated by: SCITRAN

F33657-84-D-0165

Requester: NAIC/TATA/J.M. Finley

Approved for public release; Distribution unlimited.

**Accession For**

NTIS GRA&I	<input checked="" type="checkbox"/>
DTIC TAB	<input type="checkbox"/>
Unannounced	<input type="checkbox"/>
Justification	

By

Distribution

Availability Codes

Dist

Avail and/or  
Special

THIS TRANSLATION IS A RENDITION OF THE ORIGINAL  
FOREIGN TEXT WITHOUT ANY ANALYTICAL OR EDITO-  
RIAL COMMENT STATEMENTS OR THEORIES ADVOC-  
ATED OR IMPLIED ARE THOSE OF THE SOURCE AND  
DO NOT NECESSARILY REFLECT THE POSITION OR  
OPINION OF THE NATIONAL AIR INTELLIGENCE CENTER.

PREPARED BY:

TRANSLATION SERVICES  
NATIONAL AIR INTELLIGENCE CENTER  
WPAFB, OHIO

NAIC- ID(RS)T-0398-94

Date

5 April 1995

#### GRAPHICS DISCLAIMER

All figures, graphics, tables, equations, etc. merged into this translation were extracted from the best quality copy available.

# USING OPTICAL INTERFERENCE METHODS TO MEASURE ACOUSTO-OPTICAL DEVICE THERMAL EFFECTS

/19\*

Xu Binghuo Zhao Guozhen

This article introduces methods for using optical interference methods to measure acousto-optical device thermal effects and acousto-optical deflection device test measurement results on  $\text{PbMoO}_4$  and  $\text{ZrF}_6$  glass. At the same time, it introduces good acousto-optical deviation device heat dispersion systems.

## I. Introduction

As is commonly known, when the two terminals of supersonic transducers input driving electric power, in them, there is only one small portion which is transferred to become usable acoustic energy. The remaining portion is transferred into heat energy, causing the transducer body to go up in temperature. The heat energy produced in transducers, through thermal conductors, is sent into interaction media, causing the media to produce non-uniform temperature field distributions. We took this type of phenomena and designated it thermal effects.  $\text{LiNbO}_3$  type transducer material possesses very high curie temperatures. Because of this, heat effects will not influence normal operation of  $\text{LiNbO}_3$  transducers. However, in acousto-optical media, when there are non-uniform heat fields, media indices of refraction produce non-uniform changes. The speed of sound also changes along with temperature variations. As far as the results are concerned, they are such phenomena as deflection light

---

\* Numbers in margins indicate foreign pagination.  
Commas in numbers indicate decimals.

point dispersion, deflection angle drift, as well as destruction of optical systems which have already been debugged. Because of this, acousto-optical devices are limited in a number of applications.

/20

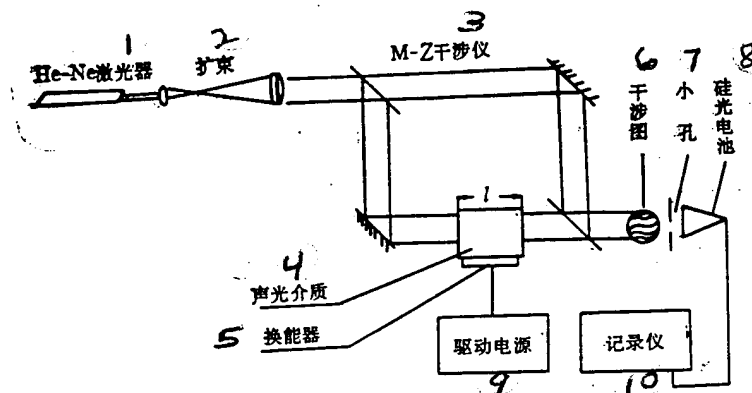


Fig.1 Schematic of Acousto-Optical Device Thermal Effect Measurement System

Key: (1) Laser (2) Expansion Beam (3) Interferometer  
 (4) Acousto-Optical Medium (5) Transducer (6) Interference Pattern (7) Small Aperture (8) Silicon Photoelectric Battery  
 (9) Motive Power Source (10) Recording Device

## II. Principles of Using Optical Interference Methods to Measure Acousto-Optical Device Thermal Effects

In order to eliminate acousto-optical device dynamic thermal effects, first of all, one should measure the dynamic temperature field distribution of the device. Outside China, people generally opt for the use of thermally sensitive components. Measuring media surface temperatures and feeding them back to control power sources, drive power is adjusted, and dynamic thermal equilibrium is reached. As far as this type of method is concerned, not only are errors relatively large, but also, it is

not possible to measure nonuniform temperature field distributions on transverse cross sections. A different type of method is to use needle hole scanning deflected light point transverse cross sections to observe macro changes in deflected light optical quality with different drive powers.

We use optical interference methods to measure transverse distributions of temperature rises on light transmitting surfaces. Fig.1 is a schematic diagram of measuring test equipment for acousto-optical device thermal effects. When a drive power source is added to transducers--due to temperature changes in media--variations occur in indices of refraction. Because of this, interference patterns move in fixed directions. We use small apertures to align any point on media transverse cross sections, measure the number of interference pattern changes at the place in question, and it is then possible to calculate the temperature changes.

In M-Z interferometers, light path errors  $S$ , which are produced due to samples being placed on one arm in them, are:

$$S = nl - l \quad (1)$$

In this,  $n$  is indices of refraction associated with acousto-optical media.  $l$  is medium length. When light path errors satisfy whole number multiples of light wave wavelengths, bright stripes appear, that is:

$$nl - l = N\lambda \quad (2)$$

In this,  $N$  is the interference order associated with interference striation patterns.  $\lambda$  is incident light wavelength. Light path changes produced due to temperature variations are

$$n \frac{\Delta l}{\Delta T} + \frac{\Delta n}{\Delta T} l - \frac{\Delta l}{\Delta T} = \frac{\Delta N}{\Delta T} \lambda \quad (3)$$

$$\frac{\Delta l}{\Delta T} (n-1) + \frac{\Delta n}{\Delta T} l = \frac{\Delta N}{\Delta T} \lambda$$

Make  $\frac{\Delta l}{\Delta T} = \frac{\Delta l}{l \cdot \Delta T} \cdot l = \alpha l$ ,  $\frac{\Delta n}{\Delta T} = \beta$  In this,  $\alpha$  are linear expansion coefficients associated with materials.  $\beta$  are indices of refraction varying with changes in temperature. It is possible to solve from among index of refraction temperature coefficients. Because of this, equation (3) can be written as:

$$[\alpha(n-1) + \beta]l = \frac{\Delta N}{\Delta T} \lambda$$

$$\therefore \Delta T = \frac{\Delta N}{\alpha(n-1) + \beta} \cdot \frac{\lambda}{l} \quad (4)$$

On the right side of equation (4), the number of interference pattern changes  $\Delta N$  is unknown.

TABLE 1 PbMoO<sub>4</sub> MATERIAL AND ZF GLASS COEFFICIENTS

① 材 料	$\alpha(\text{ppm}/^\circ\text{C})$		$\frac{1}{n} \frac{\partial n}{\partial T} (\text{ppm}/^\circ\text{C})$		$n(6328 \text{ \AA})$	
	$\alpha_{11}$	$\alpha_{33}$	② 寻常光	③ 非常光	$n_o$	$n_e$
PbMoO <sub>4</sub>	10	25	$-30 \pm 2$	$-18 \pm 2$	2.386	2.262
ZF,	8.3		6.3		1.7999	

注:  $\alpha_{11}$  为垂直于光轴方向的膨胀系数,  $\alpha_{33}$  为平行于光轴方向的膨胀系数;  $n_o$ 、 $n_e$  分别指寻常光和非常光的折射率。

Key: (1) Material (2) Ordinary Light (3) Abnormal Light  
 (4) Note:  $\alpha_{11}$  is an expansion coefficient perpendicular to the direction of the light axis.  $\alpha_{33}$  is an expansion coefficient parallel to the direction of the light axis.  $n_o$  and  $n_e$  are, respectively, indications of indices of refraction associated with normal light and abnormal light.

Besides this, all are known quantities. From this it can be seen that, in temperature change processes associated with acousto-optical media, it is only necessary to measure out variation amounts associated with interference line patterns, and it is then possible to calculate media temperature changes.

We used small 0.5mm holes aligned with any single point on the acousto-optical medium light transmitting surface and used silicon photocells and recording instruments to measure interference pattern change amounts.  $\phi 0.5\text{mm}$  small aperture areas can be seen as forming uniform temperature field distributions and uniform rises in temperature. Therefore, equation (4) can be used in order to calculate temperature changes for this small area.

Table 1 shows a number of parameters which are needed to calculate temperature changes associated with  $\text{PbMoO}_4$  materials and  $\text{ZF}_7$  glass.

### III. Heat Dissipating Structures Associated with Acousto- Optical Devices

The key to lowering thermal effects lies in dispersing as fast as possible heat produced in transducers before sending it to media. Initially, we opted for the use of  $60^\circ\text{C}$  low temperature soldering tin or electrically conductive gel lead out electrodes on transducers. With regard to this type of lead out electrode method, due to the fact that the heat source is a soldered point as well as to the fact that, on transducers, there are no heat dispersing measures, the result is the appearance of severe thermal effects. At relatively large drive powers (4W and above), sections close to transducers lose interference patterns, sometimes, even to the extent of the appearance of transducer



cracking. Later, we opted for the use of heat dissipating structures shown in Fig.2., achieving clear heat dissipation results. Their key characteristics are: (1) Electrode and transducer surface contact causes transducers to receive heat uniformly. On the upper surface of inlaid metal electrodes, several silver plates are placed, taking the divided plate transducers and connecting them up in series cascade. In conjunction with this, from the two side silver plates, there are two lead out electrodes. The thickness of the silver plates was less than 0.1mm. The size did not exceed upper electrode dimensions.

(2) Two copper pieces separated by the use of plastic net go through a very thin mica plate and silver plates in transducers, making mutual contact. A side surface of the copper plates also goes through mica plates and outer device shells making contact. Due to mica's very good thermal conductance characteristics, heat produced in transducers is immediately transmitted to two copper pieces. In this way, the heat produced in transducers goes through copper pieces and outer device shells, very rapidly dissipating. Besides this, due to mica's electrical insulation properties, it avoids short circuits through direct contact between copper pieces and four separated transducer plates.

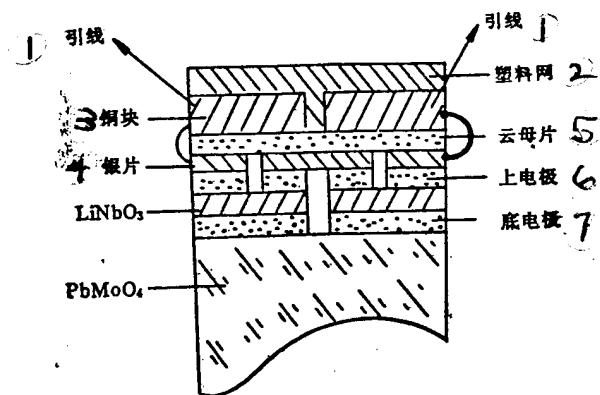


Fig.2 Copper Piece Heat Dissipation Electrode Structure

Key: (1) Lead Line (2) Plastic Net (3) Copper Piece (4) Silver Plate (5) Mica Plate (6) Upper Electrode (7) Lower Electrode

#### IV. Results of Measurements and Tests

We used optical interference methods to mainly measure thermal effects associated with  $\text{PbMoO}_4$  and  $\text{ZnF}_2$  acousto-optical deflection devices. When drive powers imputed into  $\text{TeO}_2$  acousto-optical devices were relatively low (500mW and under), thermal effects were certainly not severe. Fig.3 shows the relationships

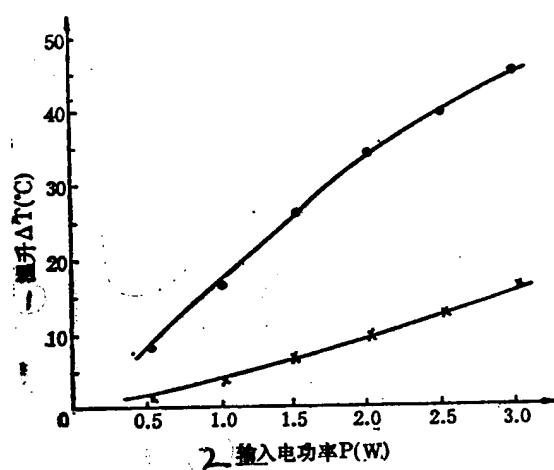


Fig.3 Relationships Between Imputed Electric Power and Acousto - Optical Media Temperature Rises Associated with Acousto-Optical Devices  
(●)--Soldered Lead Out Electrode Device (x)--Copper Piece Heat Dissipation Structure

Key: (1) Temperature Rise (2) Input Electric Power

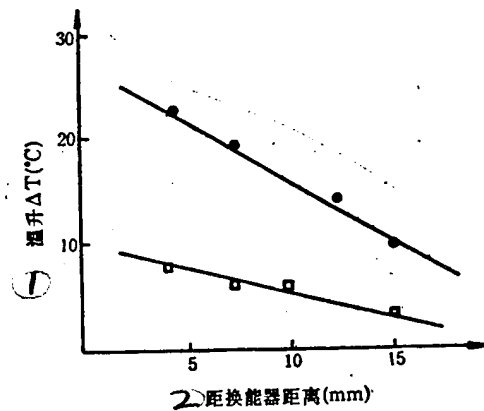


Fig.4 Temperature Rise Transverse Distribution (No.20 Device)  
 (●)--Soldered Lead Line (□)--Copper Piece Heat Dissipation

Key: (1) Temperature Rise (2) Distance from Transducer

between temperature rises and input electric power at a point 3mm from the transducer for  $\text{PbMoO}_4$  deflection devices in the two types of silver line solder and copper piece heat dissipation structures. In order to guarantee the accuracy of measurements and tests as well as to carry out comparisons under the same conditions, we used the same one piece  $\text{PbMoO}_4$  device throughout, refitting it to become copper piece heat dissipation type and silver line solder type. In measurements and tests, it was discovered that, under certain types of conditions, when the two ends of transducers add drive voltage, media temperatures very rapidly go up. However, after 5-7 min, temperature changes are not great. Because of this, in the figures, data is temperature changes associated with input electric power for 5 min. From the figures, it is possible to see that, with electric power of 2W, soldered lead out electrode device temperature rises reach approximately 30°C. However, copper piece heat dissipation structures are within 10°C.

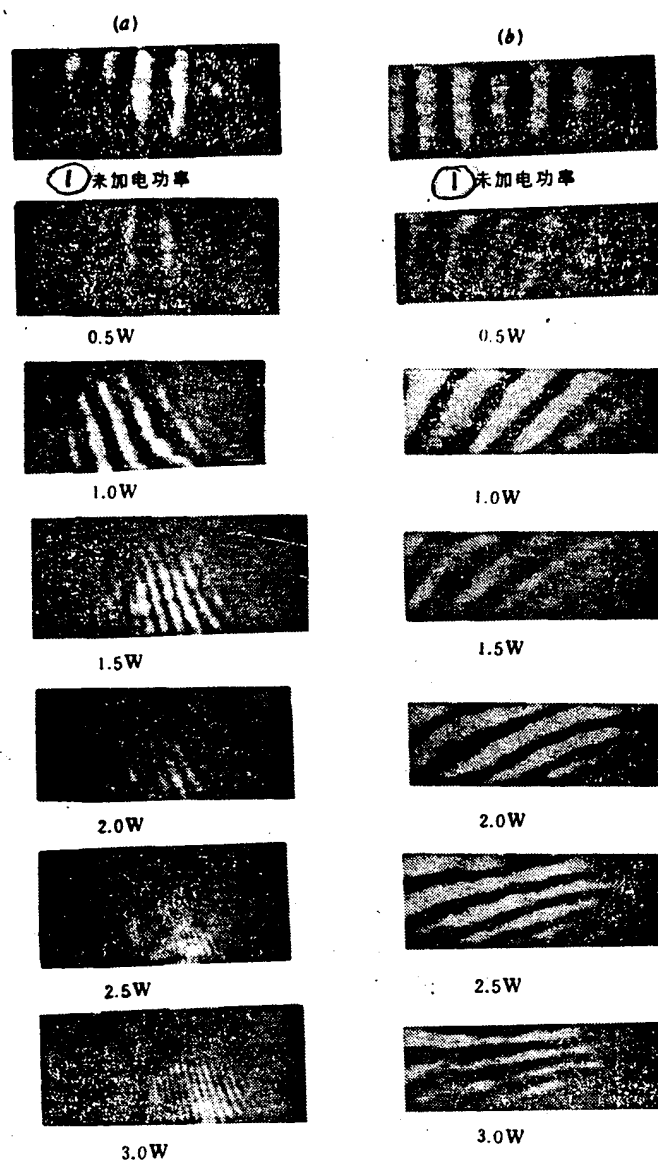


Fig.5 After 2 Minutes of Added Electric Drive Source,  
Relationships Between Interference Pattern Changes and Input  
Electric Power on  $\text{PbMoO}_4$  Crystal End Surfaces

(a) Copper Piece Heat Dissipation Structure (b) Soldered Lead  
Line Structure

Key: (1) Without Added Electric Power

Fig.4 shows, when drive power is 1.5W, transverse distributions associated with temperature rises along the direction of acoustic propagation. In sections close to transducers, due to the violence of temperature changes and interference pattern losses, using interference methods, there is no way to measure temperature changes. Because of this, when using devices, (4W or higher drive power), one should avoid using them at places 1mm-2mm from transducers. (PbMoO<sub>4</sub> modulation devices generally require 0.5W-0.8W drive power and, media temperature rises are certainly not severe).

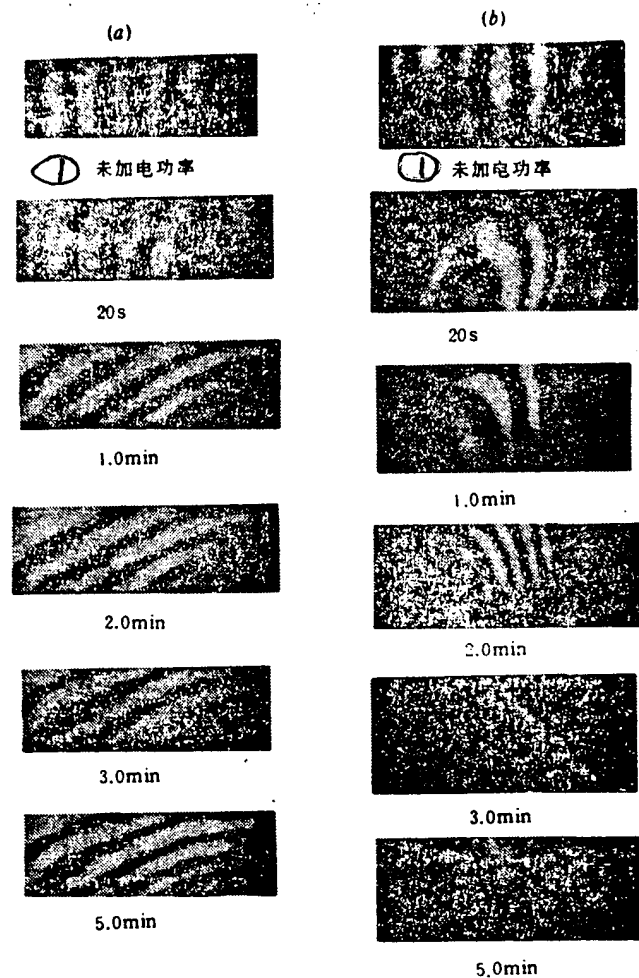


Fig.6 When Imputed Electric Power is 2W, Relationships Between Imputed Electric Power and Interference Patterns (a) Copper Piece Heat Dissipation Structure (b) Soldered Lead Line Structure

Key: (1) Electric Power Not Yet Added

We used an SB-408-B model oscilloscope camera to continuously photograph for 5 min the process of interference pattern changes. Fig.5 shows the status of interference pattern changes after 2 min of added drive voltage at different drive powers. Fig.6 shows interference pattern time changes when input power is 2W. From experiments, it can be clearly seen that interference patterns associated with soldered lead line devices move in the direction of solder points. In conjunction with this, in the vicinity of solder points, one sees the appearance of pattern distortion and close packing phenomena. In copper piece heat dissipation devices, interference patterns move in the direction of contacts along copper pieces and exterior shell. In conjunction with this, following along with increases in the duration of added voltages or increases in electric power, the direction of interference patterns gradually turns  $90^\circ$ . Finally, they become parallel to the bottom of the outer shell. The explanation of this is that heat produced in transducers really does dissipate through copper pieces and the outer shell.

## V. Discussion

If the calculation formulae associated with methodologies that use optical interference methods to measure acousto-optical device thermal effects go through a number of changes, it is possible to measure thermo-optical coefficients associated with optical glass and crystal materials. From experiments, it is clearly shown that, as far as copper piece heat dissipation methods associated with acousto-optical devices are concerned, when drive powers are 7W or less, heat dissipation results are very good. Compared to water cooling methods, they have such advantages as being relatively simpler and more easy and convenient to use. However, if drive powers exceed 7W-- particularly, if they are above 10W (for example, adjustable Q devices), opting for the use of water cooling systems is somewhat better.

DISTRIBUTION LIST

DISTRIBUTION DIRECT TO RECIPIENT

<u>ORGANIZATION</u>	<u>MICROFICHE</u>
B085 DIA/RTS-2FI	1
C509 BALL0C509 BALLISTIC RES LAB	1
C510 R&T LABS/AVEADCOM	1
C513 ARRADCOM	1
C535 AVRADCOM/TSARCOM	1
C539 TRASANA	1
Q592 FSTC	4
Q619 MSIC REDSTONE	1
Q008 NTIC	1
Q043 AFMIC-IS	1
E051 HQ USAF/INET	1
E404 AEDC/DOF	1
E408 AFWL	1
E410 AFDTC/IN	1
E429 SD/IND	1
P005 DOE/ISA/DDI	1
P050 CIA/OCR/ADD/SD	2
1051 AFIT/LDE	1
PO90 NSA/CDB	1
2206 FSL	1

Microfiche Nbr: FTD95C000170  
NAIC-ID(RS)T-0398-94